Surface Waves Generated on Electrolytes by a Traveling Electromagnetic Force

Gerardo Alcalá and Sergio Cuevas

Abstract This paper presents an experimental study of gravity-capillary waves generated at the free surface of a thin-film of electrolyte ($NaHCO_3$) due to the presence of an electromagnetic force created by the interaction of a direct electric current and a traveling magnetic field.The field is generated by a permanent magnet moving in straight line, localized externally to the bottom wall of the fluid container. The dominant component of the magnetic field is perpendicular to the plane of the fluid surface in equilibrium. The current is applied transversely to the motion of the magnet through a pair of parallel electrodes, in such a way that the force points either in favour or against the motion of the magnet, depending on the polarity of the electrodes and the magnet orientation. A vertical force component is also generated near the edges of the magnet. It is shown that the electromagnetic force acts as an obstacle for the flow (a *magnetic obstacle*) and, similarly to a moving solid object, it is able to generate a stationary wave pattern. This patten is reconstructed by optical methods for several magnet velocities. Differences produced by the force acting in favour or against the magnet motion are discussed.

1 Introduction

Surface waves are a common phenomenon in nature. In many situations they are generated by obstacles interacting with the free surface as occurs, for instance, when a stone is dropped in a pond, a duck swims at the surface of a lake, or a river flow passes through a fishing line, among many other situations. Such waves establish a competition between gravity and surface tension, and the equilibrium shape taken by the surface of the fluid is a consequence of this balance (Landau and Lifshitz 1959).

G. Alcalá (✉) · S. Cuevas
Instituto de Energias Renovables, Universidad Nacional Autónoma de México,
A.P. 34, 62580 Temixco, Morelos, México
e-mail: gealp@ier.unam.mx

J. Klapp and A. Medina (eds.), *Experimental and Computational Fluid Mechanics*,
Environmental Science and Engineering, DOI: 10.1007/978-3-319-00116-6_32,

In the present work, we are interested in the experimental study of capillary-gravity waves generated by localized electromagnetic forces that act as *obstacles* for the flow. In a biological context capillary-gravity waves are involved in the mechanisms of locomotion, hunting or courtship for insects or arachnids (Bush and Hu 2006; Bleckmann and Bender 1987). On the other hand, magnetic fields can be used for the control of surface waves in different metallurgical applications (Sreenivasan et al. 2005). Before addressing the analysis of capillary-gravity waves created by electromagnetic forces, we recall some important features of surface waves generated by solid obstacles.

When an object partially immersed in a fluid is moving uniformly, it will experience drag forces acting on it. Different contributions to the drag or resistance forces can be identified (Burghelea and Steinberg 2002). In fact, in addition to the common viscous resistance, R_f, an eddy resistance, R_e, caused by either laminar or turbulent wakes will be present. But the generation of capillary-gravity waves can also contribute to another form of resistance called *wave resistance*, R_w, which represents the momentum removed by the waves from the object and taken away to infinity (Havelock 1919). Due to the viscosity of water and electrolytes, usually R_f and R_e can be considered negligible compared with the capillary-gravity wave resistance (Shliomis and Steinberg 1997).

In the frame of an object moving in the fluid with velocity $\mathbf{U}$, we will observe a stationary wave pattern where the wave speed, c, satisfies the following condition (Lighthill 1979)

$$c(\mathbf{k}) = U \cos\theta(\mathbf{k}), \tag{1}$$

where $\mathbf{k}$ is the wave vector and θ is the angle between $\mathbf{U}$ and $\mathbf{k}$, so that the component $U \cos\theta$ of the object velocity, at right angles to the crest, can cancel the crest's motion at the wave speed c.

In general, due to the dispersive nature of the capillary-gravity waves, complex surface structures will be observed. By neglecting viscous effects, the phase velocity, c, can be expressed by the following equation

$$c = \left[\tanh kh\,(g/k + \gamma k/\rho)\right]^{1/2}, \tag{2}$$

where ρ is the fluid density, γ is the liquid-air surface tension, g is the gravitational acceleration, h is the fluid depth, and k is the wave number (Acheson 1990). As we can see, the velocity c depends on the wavelength, so that among all wavelengths, Eq. (1) fixes some of them which can be stationary.

According to Eq. (2), for deep waters ($kh \gg 1$) phase velocity has a minimum $c_c = (4g\gamma/\rho)^{1/4}$ at the capillary wave number $\kappa = \sqrt{\rho g/\gamma}$. For water at room temperature, we have $c_c = 23$ cm/s and $\lambda_c = 1.7$ cm, where λ_c is the wavelength. This means that Eq. (1) cannot be satisfied for $U < c_c$, and no such waves can be present for a slow moving object. In fact, some waves will be found upstream and some others downstream the obstacle, which is related with the way the energy is propagated.

Now, let us consider a frame of reference moving with the stream and an obstacle traveling with velocity U in the upstream direction. The longer waves generated by the motion of the object, with wave speed $c = U$, greater than the energy propagation (group) velocity c_g, are then left behind the obstacle and travel in the downstream direction. In other words, after energy is generated, the long waves lag behind the object. Shorter waves, for which $c = U$ is smaller than c_g, will be found ahead of the obstacle (Lighthill 1979). The case of surface waves generated by objects of small size, relative to the capillary length $\kappa^{-1} = (\gamma/(\rho g))1/2$, has also been considered by many authors Raphaël and deGennes (1996); Richard and Raphael (1999); Sun and Keller (2001); Chepelianskii et al. (2008); Closa et al (2010); Le Merrer et al. (2011). Let us now consider surface waves generated by a localized electromagnetic force.

2 Waves Generated by Electromagnetic Forces

In this paper, we show that localized electromagnetic forces are an alternative to the use of solid obstacles for generating surface waves in electrically conducting fluids. In fact, it has been shown that when a uniform flow of a highly conducting fluid (*v.e.* a liquid metal) passes through a localized non-homogenous magnetic field, for instance produced by a dipolar permanent magnet, the field acts in a similar way as a solid obstacle by deflecting the incident flow and generating a wake behind the magnetic field spot (Cuevas et al. 2006; Votyakov et al. 2007; Votyakov and Kassinos 2009). In this case, the currents induced by the relative motion of the liquid and the magnetic field interact with the applied field producing an opposing Lorentz force $\mathbf{j} \times \mathbf{B}_0$, where $\mathbf{j}$ is the induced current density and $\mathbf{B}_0$ is the applied field. Therefore, it is possible to conceive the localized magnetic field as an obstacle for the flow; incidentally, the term *magnetic obstacle* was coined for that purpose (Cuevas et al. 2006). It has to be mentioned, however, that flows past solid and magnetic obstacles present very important differences.

If the conducting fluid is an electrolyte, induced currents are negligibly small and in order to observe the effect of a localized magnetic field in an electrolytic flow, an external current, $\mathbf{j}_0$, has to be applied. In fact, experiments of flows of electrolytes past localized magnetic fields have been performed by dragging an external permanent magnet at constant velocity close to a quiescent thin layer of electrolyte, while a steady current was imposed on the fluid layer transversely to the motion of the magnet (Honji 1991; Honji and Haraguchi 1995; Afanasyev and Korabel 2006). In these studies, the attention was focused on the velocity patterns created in flow planes parallel to the bottom wall, while the effects of the localized Lorentz force on the free surface of the electrolyte were completely disregarded. Here, we are interested in studying flow regimes where three-dimensional effects produced by localized Lorentz forces are able to perturb the free surface and generate surface wave patterns.

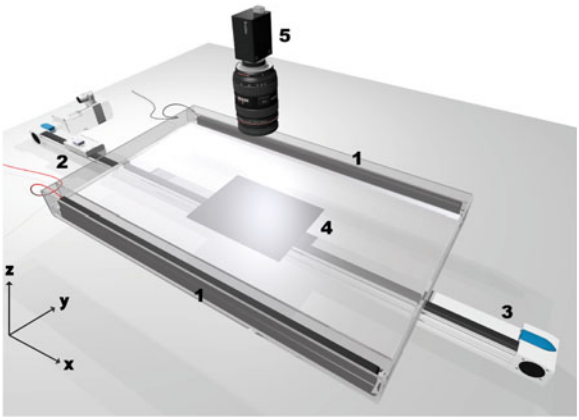

Fig. 1 Experimental setup. A localized Lorentz force is created by the interaction of a D.C. current applied through parallel electrodes (1) and the field of a permanent magnet (2) dragged axially outside the bottom wall with a linear actuator (3). The perturbed free surface is reconstructed at the observation zone (4) with the aid of a camera (5), using the synthetic Schlieren method (Moisy et al. 2009)

3 Experimental Setup and Procedure

A sketch of the experimental setup is shown in Fig. 1. The experiments were conducted in a rectangular crystal tank (35 cm $\times$ 60 cm $\times$ 5 cm), set horizontally and filled with a 8.6% aqueous electrolytic solution of $NaHCO_3$ up to the depth of 3 mm. Two electrodes (square graphite rods of 1 cm $\times$ 1 cm of cross-section and 50 cm in length) were placed along the two long sides of the container and connected to a power supply that provided a constant voltage of 60 V, so that a direct electric current (D.C.) of 2 A circulated in the fluid layer in the transversal direction. Electrodes were inside chambers (*bubble traps*) that allow the electric current to flow at the bottom while preventing the bubbles to invade the main flow region. A square permanent magnet of side length $L = 2.54$ cm, located below the bottom wall of the tank, was moved along the symmetry axis of the tank at a constant speed, U, using a linear actuator (FESTO EGC-70-500-TB-KF-0H-GK) driven by a servo motor (FESTO EMMS-AS-70-M-RS), in which U can be carefully controlled. In the experiment, starting at rest, the manget was suddenly set in motion reaching a constant velocity before it enters below the tank. The interaction of the D.C. current and the localized magnetic field of the traveling magnet, produced a Lorentz force that perturbed the free surface and generated a wave pattern. The Lorentz force also affected the bulk flow but this is not analyzed here.

Since the main component of the magnetic field is normal to the bottom wall and the applied current is transversal to the motion of the magnet, the Lorentz force points either in the direction of the motion of the magnet or against it, depending on the polarity of the electrodes and the orientation of the permanent magnet. If the polarity of the electrodes (*i.e.* the direction of the current) is fixed, the force direction

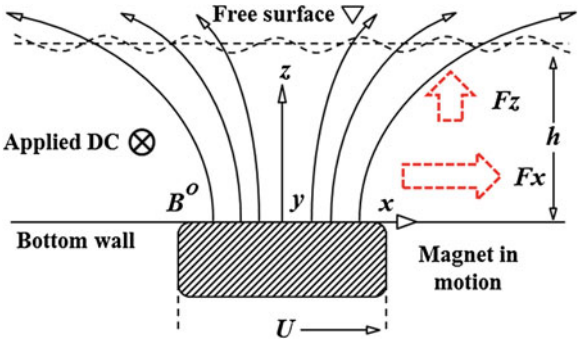

Fig. 2 Sketch of the physical situation when the north pole of the traveling magnet (moving to the *right* with speed U) is oriented upwards and the transversal current enters the plane of the figure. In this case, one component of the localized Lorentz force points in the direction of the motion of the magnet and another points vertically

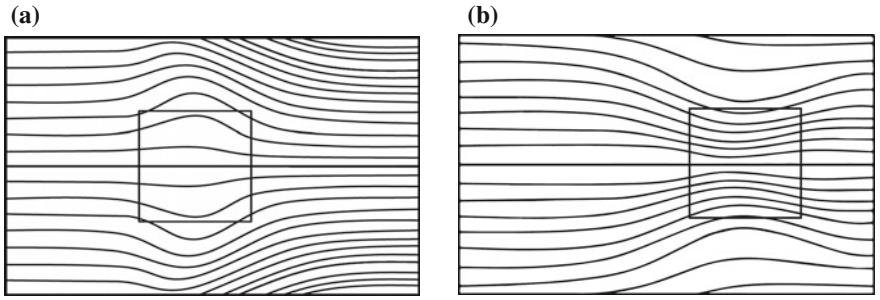

Fig. 3 *Top* view of streamlines in the flow of an electrolyte past a localized magnetic field (represented by the *square*). Streamlines expand for a positive force and contract for a negative one. **a** Positive force. **b** Negative force

depends only on the magnet orientation (see Fig. 2). Let us call *positive force* the case when the horizontal component of the Lorentz force points in the direction of the motion of the magnet, and *negative force* when it points against the motion of the magnet. For a positive force the streamlines expand around the region affected by the localized magnetic field, while for the other case the streamlines contract in this region, as shown in the Fig. 3a, b, respectively. Notice that the effects of a positive force are similar to those of a solid object while the effects of a negative force have no mechanical analogy. We have to consider, however, that near the magnet borders the component of the field in the axial direction gives rise to a Lorentz force component in the vertical direction that is able to perturb the free surface. In fact, the strength of the perturbation depends on the velocity of the magnet.

Two relevant dimensionless numbers can be identified in this problem. First, the Reynolds number, $Re = UL/\nu$, based on the speed of the magnet U, the side length of the magnet L, and the kinematic viscosity of the fluid ν. Secondly, the Lorentz force

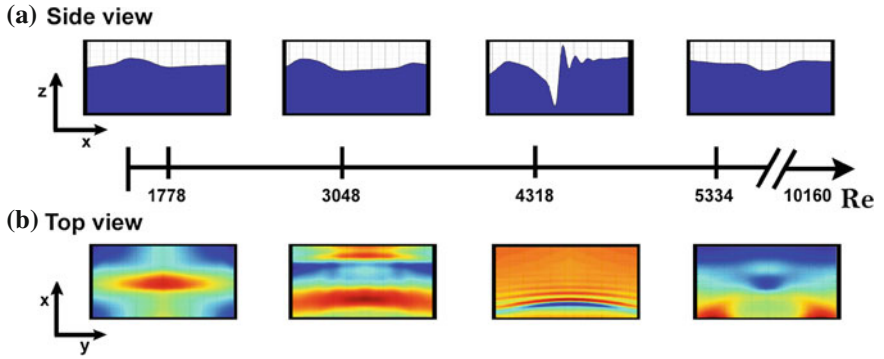

Fig. 4 Wave patterns for a positive force for different Reynolds numbers. **a** *Vertical* wave patterns profiles at the mid symmetry plane. **b** *Horizontal* proyection of free surface topography

parameter defined as $Q = j_0 B_{max} L^3/\rho\nu^2$ where j_0 is the applied current density, B_{max} is the maximum strenght of the magnetic field at the surface of the magnet, and ρ is the mass density. The experiments reported in this work were conducted by fixing the value of Q and varying Re.

The wave pattern generated by the traveling localized magnetic force is stationary with respect to the system of the magnet moving with velocity U. The stationary wave patterns were characterized experimentally over a 10 cm $\times$ 10 cm region using an optical method called *free surface synthetic Schlieren* (Moisy et al. 2009). This method allows the measurement of the instantaneous topography of the interface between two transparent fluids. In order to implement this technique, a camera located above the tank with the fluid at rest (see Fig. 1) records an aleatory dot pattern placed below the transparent bottom wall. When the free surface is perturbed, an apparent motion of the dots is observed due to refraction. By using a digital image correlation (DIC) algorithm to measure the apparent displacement field between the refracted image and the reference image obtained when the surface is flat, it is possible to calculate the height, h, of the free surface by solving the following equation

$$\nabla h = -\frac{\mathbf{r}}{h^*}, \tag{3}$$

where $\mathbf{r}$ is the displacement and the effective distance h^* is a constant that depends on the refraction indexes and thicknesses of different media (air, glass, and the electrolyte) through which light travels from the dots to the camera.

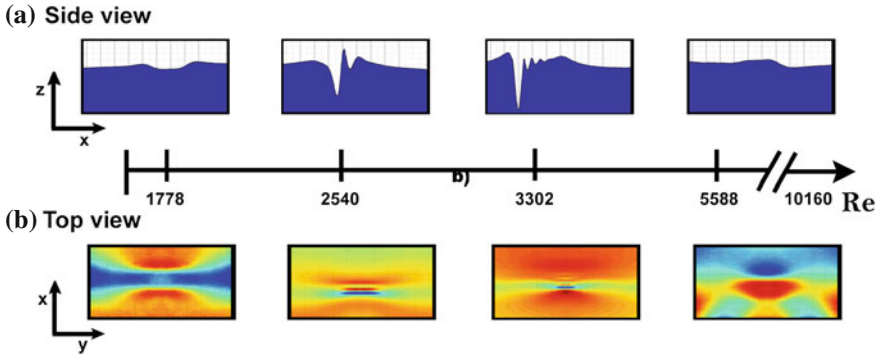

Fig. 5 Wave patterns for a negative force for different Reynolds numbers. **a** *Vertical* wave patterns profiles at the mid symmetry plane. **b** *Horizontal* proyection of free surface topography

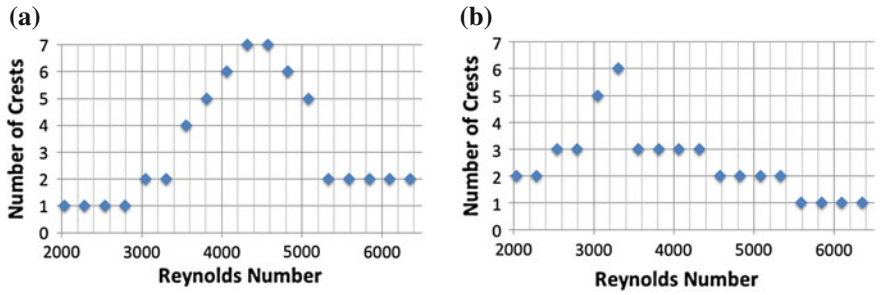

Fig. 6 Variation of the number of crests with *Re* due to emission of capillary-gravity waves. **a** Positive force. **b** Negative force

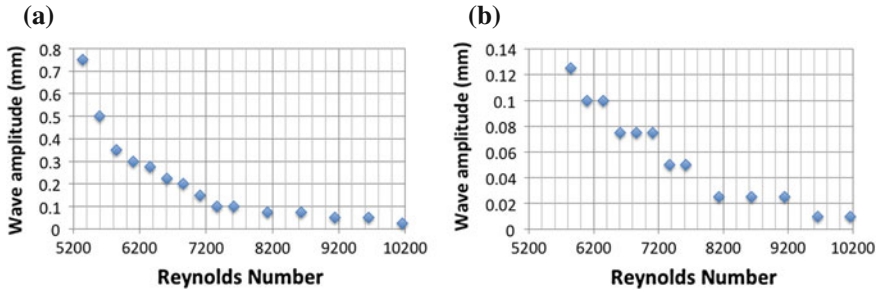

Fig. 7 Amplitude of the persisting wave in the large Reynolds number range as a function of *Re*. **a** Positive force. **b** Negative force

4 Experimental Results

Experiments were performed for a constant value of the Lorentz force parameter ($Q = 5.2$) while the Reynolds number, Re, varied from 1778 to 10160. In Figs. 4 and 5, the evolution of wave patterns for the cases of positive and negative forces, respectively, is illustrated schematically for growing Reynolds. In the upper panels (Figs. 4a and 5a), a side view of the vertical central plane that crosses the axial symmetry axis shows the wave pattern profiles created by the Lorentz force. In turn, the lower panels (Figs. 4b and 5b) show a projection of the topography of the free surface in the horizontal plane, where the color scale indicates different hights of the surface. Maximum wave amplitudes were 1.5 and 0.8 mm for positive and negative forces, respectively.

For a positive force, a dominant crest is observed in the low Re regime ($1778 \leq Re \leq 2794$). For higher Re, short waves appear in the front due to emission of capillary-gravity waves. Wave emission is observed within the range $3048 \leq Re \leq 5080$. In fact, the number of crests increases as Re increases up to reaching a maximum number of seven for an intermediate value ($Re \approx 4318$). This is shown in Fig. 6a, where the number of crests is plotted versus the Reynolds number for the positive force case. When Re is increased further, the number of crests decreases. Finally, in the high Re regime ($5334 \leq Re \leq 10160$), only a pair of crests can be identified, corresponding to a dominant valley that persists in this range of Re (see Fig. 6a). The depth of this valley decreases as Re grows. In Fig. 7a, the amplitude of the wave associated with the dominant valley is shown as a function of Re. It can be observed a sharp decrease of the amplitude from 0.8 mm for $Re = 5334$ up to practically disappearing for $Re = 10160$.

In the case of a negative force, a dominant valley is found for low Re ($2032 \leq Re \leq 2286$). As the Reynolds number increases, wave emission appears and the number of crests increases. Wave emission was observed in the range $2540 < Re < 5334$ and a maximum number of six crests was found for $Re \approx 3302$ (see Fig. 6b). As Re decreases, the number of crests reduces first to three ($3556 \leq Re \leq 4318$), then to two ($4572 \leq Re \leq 5334$), and finally to one ($5588 \leq Re \leq 10160$), indicating the dominant crest that appears in the higher range of Re explored (Fig. 6b). Figure 7b shows the amplitude of the wave associated with the dominant crest as a function of Re. In fact, the original amplitude (0.13 mm for $Re = 5842$) is much smaller than in the positive force case and similarly, decreases up to practically disappearing for $Re = 10160$.

5 Concluding Remarks

The generation of surface waves through localized traveling electromagnetic (Lorentz) forces in a thin layer of electrolyte was analyzed experimentally. The Lorentz force was created by the interaction of a direct electric current applied

transversally to the motion of a permanent magnet external to the fluid container. In this work, it was shown that the localized Lorentz force acts as a magnetic obstacle that is able to generate not only vortical flows, as has been demonstrated by previous investigations (Honji 1991; Honji and Haraguchi 1995; Afanasyev and Korabel 2006), but also to perturb the free surface and produce free surface wave patterns. The instantaneous topography of the surface was reconstructed using the free surface synthetic Schlieren method (Moisy et al. 2009). The evolution of the wave patterns was characterized as a function of the Reynolds number (based on the velocity of the traveling magnet), while the Lorentz force parameter, Q, remained fixed. The Reynolds number varied from 1778 to 10160. In contrast with surface waves generated by moving solid obstacles, the Lorentz force can point either in favour (positive force) or against (negative force) the motion of the traveling magnetic field, depending on the orientation of the magnet and the direction of the applied current. In fact, the observed wave patterns differ according to the direction of the Lorentz force. It was found that, as the Reynolds number increases, there is a transition regime where short capillary-gravity waves are created by the localized electromagnetic force. For a positive force the transition goes from a dominant crest in the low Reynolds number regime to a dominant valley in the high Reynolds number regime. For a negative force, the transition occurs inversely from a dominant valley to a dominant crest. Emission of capillary-gravity waves starts at smaller Reynolds numbers in the case of a negative force. For both positive and negative forces, the amplitude of the persistent wave in the high Reynolds number regime was found to decrease and almost disappear as Re reached the largest explored value.

Acknowledgments This work has been supported by CONACyT, Mexico, under project 131399. G. Alcalá also acknowledges a grant from CONACyT.

References

Acheson DJ (1990) Elementary fluid dynamics. Clarendon Press, Oxford
Afanasyev YD, Korabel VN (2006) J Fluid Mech 553:119
Bleckmann H, Bender M (1987) J Arachnol 15:363–369
Burghelea T and Steinberg V, (2002) Phys Rev E **66**(5)
Bush JWM, Hu DL (2006) Annu Rev Fluid Mech 38:339–369
Chepelianskii A, Chevy F and Raphaël E, (2008) Phys. Rev. Lett. **100**(7)
Closa F, Chepelianskii AD, Raphaël E (2010) Phys Fluids **22**(5)
Cuevas S, Smolentsev S, Abdou MA (2006) J Fluid Mech 553:227–252
Havelock T H, (1919) Proc R Soc London A Math Phys Sci **95**(670):354–365
Honji H (1991) J Phys Soc Japan 60(4):1161–1164
Honji H, Haraguchi Y (1995) J Phys Soc Jpn 64(7):2274–2277
Landau LD, Lifshitz EM (1959) Fluid mechanics. Pergamon Press, Oxford
Le Merrer M, Clanet C, Quere D, Raphaël E, Chevy F (2011) Proc Nat Acad Sci **108**(37):15064–15068
Lighthill J (1979) Waves in fluids, 6th edn. Cambridge University Press, Cambridge
Moisy F, Rabaud M, Salsac K (2009) Exp Fluids 46(6):1021–1036

Raphaël E, deGennes PG (1996) Phys Rev E 53(4):3448–3455
Richard D, Raphael E (1999) Europhys Lett 48(1):49–52
Shliomis MI, Steinberg V (1997) Phys Rev Lett 79(21):4178
Sreenivasan B, Davidson PA, Etay J (2005) Phys Fluids 17:117101
Sun SM, Keller JB (2001) Phys Fluids 13(8):2146
Votyakov EV, Zienecke E, Kolesnikov YB (2008) J Fluid Mech 610:131–156
Votyakov EV, Kassinos SC (2009) Phys Fluids 21:097102